Original Research Article

Land Use Land Cover Classification of Burhner River Watershed Using Remote Sensing and GIS Technique

ABSTRACT

Information on Land Use Land Cover (LULC) pattern is very important for developing management strategies for land use planning. Remotely sensed satellite data has proved to be an unmatched source of information that can deliver LULC information with good accuracy especially in regions where acquiring LULC information through intensive ground surveys seems to be impractical. The present study aims at performing LULC classification of Burhner river watershed situated in Mandla, Balaghat and Dindori districts of Madhya Pradesh, India. Sentinel-2B satellite imagery with spatial resolution of 10 m was used in the present investigation. A total number of 6 LULC classes were identified in the study area namely agricultural land, fallow/open land, forest, habitation, wasteland and waterbodies using ERDAS IMAGINE® 2011. Accuracy assessment of the LULC classified image from reference (ground truth) data using error matrix revealed an overall accuracy of 95.72% with kappa coefficient of 0.94. Furthermore, the error matrix also aided in computing classified image producer's and user's accuracy which were under acceptable limits. The LULC statistics of study area indicated that highest area is covered by forest (53.01%), followed by fallow/open land (24%), agricultural land (19.44%) and least area is covered by waterbodies (1.38%) and habitation (0.19%). A major portion of study area under fallow/open land category pointed that underutilized land resource potential exist in watershed. Such land can be further utilized for crop production and plantation purposes in order to maximize output from the available natural resources in a sustainable manner.

Keywords: Land use land cover classification, digital image processing, accuracy assessment, remote sensing, geographic information system.

1. INTRODUCTION:

The land surface is used for a variety of purposes. It possesses various characteristics over its spatial extent with a period [1,2]. Land surface undergo dynamic changes resulting from natural and human induced activities [3,4]. The human induced activities are attributed to increase in human population, agricultural expansion, and changes in socio-economic well-being of the people which have triggered unsustainable extraction of natural resources [5,6,7]. The ever growing population and limited availability of land necessities proper utilization of available land through scientific land use planning [8,9,10].

Accurate and timely monitoring of land through Land Use Land Cover (LULC) mapping plays a critical role in a variety of sectors in the developing world including food security, land use planning, hydrology modeling and natural resources management [11]. LULC classification is a hybrid type of classification [2,12]. The terms land use and land cover have some fundamental differences [13, 14] and thus it becomes essential to define them clearly. Land cover represents the observed biophysical cover of the Earth's surface whereas land use describe the arrangements, activities and inputs people undertake within a particular land type to produce, modify and maintain it [15]. Land use is an expression of human activity developed for social, economic, cultural and political purposes [16].

LULC monitoring at watershed scale holds a significant role in scientific investigations as it aims to identify the risk associated from land resources degradation, watershed deterioration and ecosystem instability [17]. A watershed is an area from which runoff resulting from precipitation flows past a single point into large stream, river, lake or ocean [18,19]. Watersheds play a crucial role in natural functioning of Earth thus considered as a core planning unit for sustainable management of natural resources (*i.e.,* land and water) [20].

Advances in remote sensing science and associated technologies have made it possible to obtain the valuable spatiotemporal information on LULC [21]. Remotely sensed satellite imagery and image classification methods provide cost effective and accurate means to derive LULC information [22]. Remote sensing has become a vital source of information for natural resources management including LULC mapping. With the advent of remote sensing and Geographical Information System (GIS) technologies, the monitoring of LULC pattern and change detection are now made possible at low cost and with better accuracy [23, 24, 25].

Several studies have been successfully conducted in past delivering accurate LULC information using remotely sensed satellite data [14, 21, 26]. Sharma et al., [27] performed LULC classification of Gusuru river watershed situated in Satna and Panna districts of Madhya Pradesh with an overall accuracy of 88.03%. Patle et al., [28] executed LULC classification of Nahra nala watershed situated in Balaghat district of Madhya Pradesh, India with an overall classification accuracy of 95.52% and kappa coefficient of 0.92.

The integrated use of remote sensing and GIS techniques can provide accurate information of LULC pattern with much ease as compared to the traditional ground based surveys [29]. Keeping all such perspectives in mind, the present study aims to perform LULC classification of Burhner river watershed situated in Mandla, Balaghat and Dindori districts of Madhya Pradesh using remote sensing and GIS techniques.

2. MATERIAL AND METHODS:

2.1 Study area:

The Burhner river rises from the Maikala range, south-east of Gwara village in Mandla district of Madhya Pradesh, India. The Burhner river watershed is geographically located between 80°34'40"E to 81°23'20"E longitudes and 22°49'45"N to 22°31'00"N latitudes coinciding with Mandla, Balaghat and Dindori districts of Madhya Pradesh. The elevation in watershed varies from 393 to 954 m above M.S.L. (Mean Sea Level) with total watershed area of 3959.813 km². The study area receives majority of its rainfall from southwest monsoon from June to September. The normal annual rainfall in watershed is 1647.8 mm/year [30, 31]. The location map of the study area is illustrated in Fig. 1.

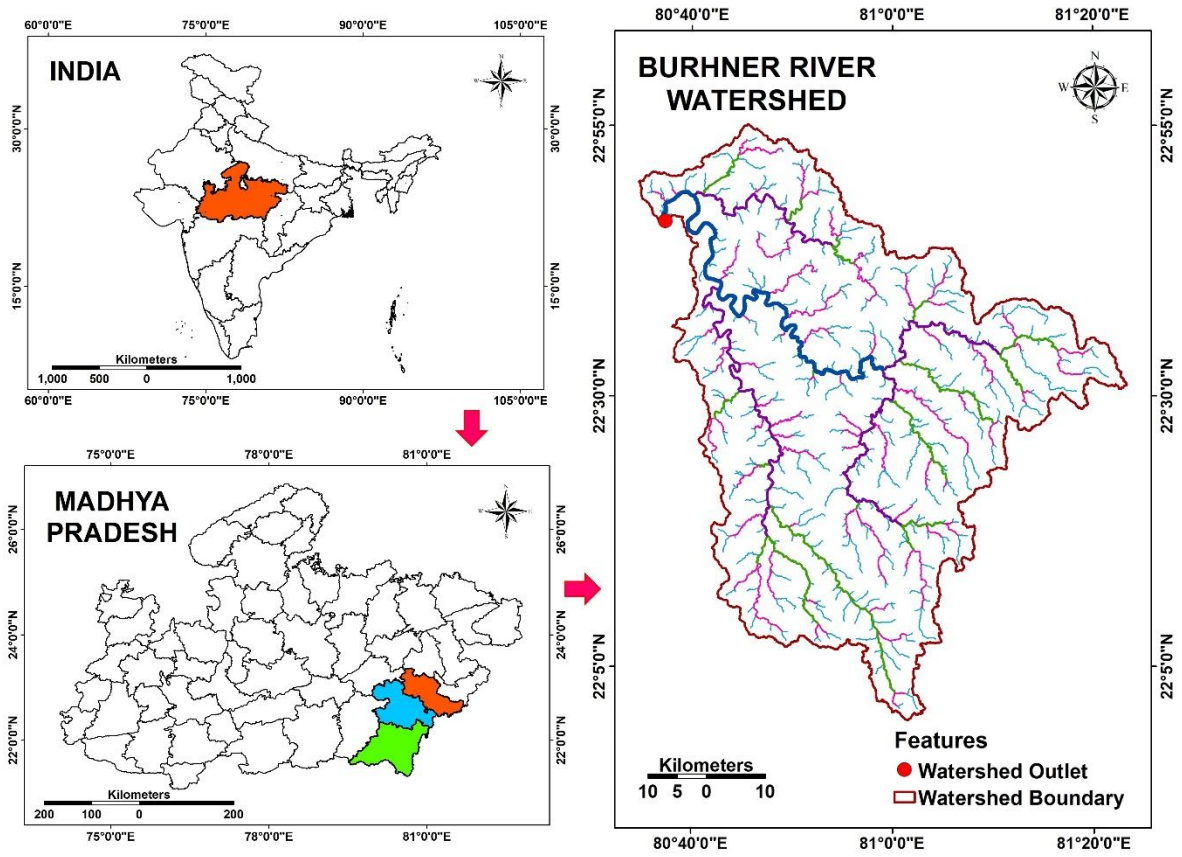

Fig. 1 Location map of study area

2.2 Data source and methodology:

The digital topographic data used in the present study aided in correct delineation of watershed boundary. The delineation was executed by utilizing CARTOSAT DEM (Digital Elevation Model) of 30 m spatial resolution. The CARTOSAT DEM was acquired from Bhuvan ISRO's Geoportal with its URL as https://bhuvan-app3.nrsc.gov.in/data/download/index.php. The delineation was done by using snap pour point methodology in ArcGIS® 9.3 environment. The DEM tiles were initially pre-processed by mosaicking the tiles and were re-projected to a common and widely used UTM (Universal Transverse Mercator) projected coordinate system (Zone 44N) with WGS (World Geodetic System) 1984 as geographic coordinate system. A series of GIS operations such as fill sinks, flow direction, flow accumulation available under spatial analyst tool of Arc toolbox were followed with subsequent designation of watershed outlet so as to obtain the watershed boundary. The resultant watershed boundary was further verified with its base map.

For preparing the base map of the study area, a total number of 14 toposheets coinciding with the study area were used. Survey of India (SOI) toposheets with toposheets number as 64B/9, 64B/10, 64B/11, 64B/12, 64B/13, 64B/14, 64B/15, 64B/16, 64F/2, 64F/3, 64F/4, 64F/6, 64F/7 and G4G/1 with a scale of 1:50,000 procured from SOI Nakshe Portal (URL: https://soinakshe.uk.gov.in) were used.

To prepare the LULC thematic map of the study area, a cloud free remote sensing based satellite imagery of Sentinel-2B Level 1C MSI (Multi Spectral Instrument) with spatial resolution of 10 m freely downloaded from United States Geological Survey (USGS) Earth Explorer website (URL: https://earthexplorer.usgs.gov) was used. The date of acquisition of the imagery was 18 January 2021 and a total number of 4 tiles with tile name as T44QMK, T44QML, T44QNK, T44QNL together coinciding with watershed boundary were used. The procured tiles were having projected coordinate system as UTM Zone 44N and geographic coordinate system as WGS 1984. The bands of acquired

image came with JPEG2000 file extension. Table 1 shows brief information of spatial and spectral characteristics of bands used in Sentinel-2B MSI [28].

Table 1. Brief details of spatial and spectral characteristics of bands used in Sentinel-2B MSI

Band	Spatial resolution (m)	Wavelength (µm)	Description
Band 1	60	0.443	Ultra-Blue-Coastal and Aerosol
Band 2	10	0.490	Blue
Band 3	10	0.560	Green
Band 4	10	0.665	Red
Band 5	20	0.705	Visible and Near Infrared (VNIR) – Vegetation Red Edge 1
Band 6	20	0.740	Visible and Near Infrared (VNIR) – Vegetation Red Edge 2
Band 7	20	0.783	Visible and Near Infrared (VNIR) – Vegetation Red Edge 3
Band 8	10	0.842	Near Infrared (NIR)
Band 8A	20	0.865	Narrow Near Infrared (NNIR)
Band 9	60	0.945	Short Wave Infrared (SWIR) – Water vapour
Band 10	60	1.375	Short Wave Infrared (SWIR) – Cirrus
Band 11	20	1.610	Short Wave Infrared (SWIR)
Band 12	20	2.190	Short Wave Infrared (SWIR)

2.3 LULC Classification approach:

At the initial stage, pre-processing technique (*i.e.,* atmospheric correction) was applied to the tiles in order to generate reflectance files using ERDAS IMAGINE® 2011. The band 2 (blue), band 3 (green), band 4 (red) and band 8 (NIR) as obtained after atmospheric correction were further used to prepare the RGB composite image for each tile. The RGB composite image was prepared by using the layer stack tool available in ERDAS (Earth Resources Data Analysis System) IMAGINE® 2011 which is a most preferred and widely used digital image processing software. The RGB composite tiles were mosaicked and further made subset by using vector file of watershed boundary. The change in band combination of RGB composite image successfully yielded FCC (False Colour Composite) image. A false colour composite image is one in which the red, blue and green values do not correspond to the true colours of red, green and blue. The most commonly used FCC image displays the near infrared as red, red as green and green as blue. Thus, FCC can be defined as an artificially generated colour image in which the red, green and blue colours are assigned to the wavelength in which they do not belong in nature. The False Colour Composite (FCC) image of the study area is shown in Fig. 2

The FCC image of the study area aided in preparing the AOI (Area of Interest) files of different LULC classes using on-screen visual interpretation principles (Fig. 3), available ancillary data, prior knowledge-based logic rules, sufficient ground truth (reference) data (Fig. 4) and satellite data of Google Earth Pro. After preparation of AOIs, unsupervised classification was performed using FCC image that yielded broad classes of LULC in the classified image. The obtained image was recoded to prominent LULC classes characterized by variations in tone, texture, shape, association, and the pattern of various objects within the satellite data. A total of six prominent LULC classes *viz.,* agricultural land, fallow/open land, forest, habitation, waste land and waterbodies were identified during the classification process. Subsequently, the AOI files were further overlaid on unsupervised classified image to get thematically recoded raster image. At last, area covered by each LULC class covered was calculated. The methodological framework used in the classification approach is shown in Fig. 5.

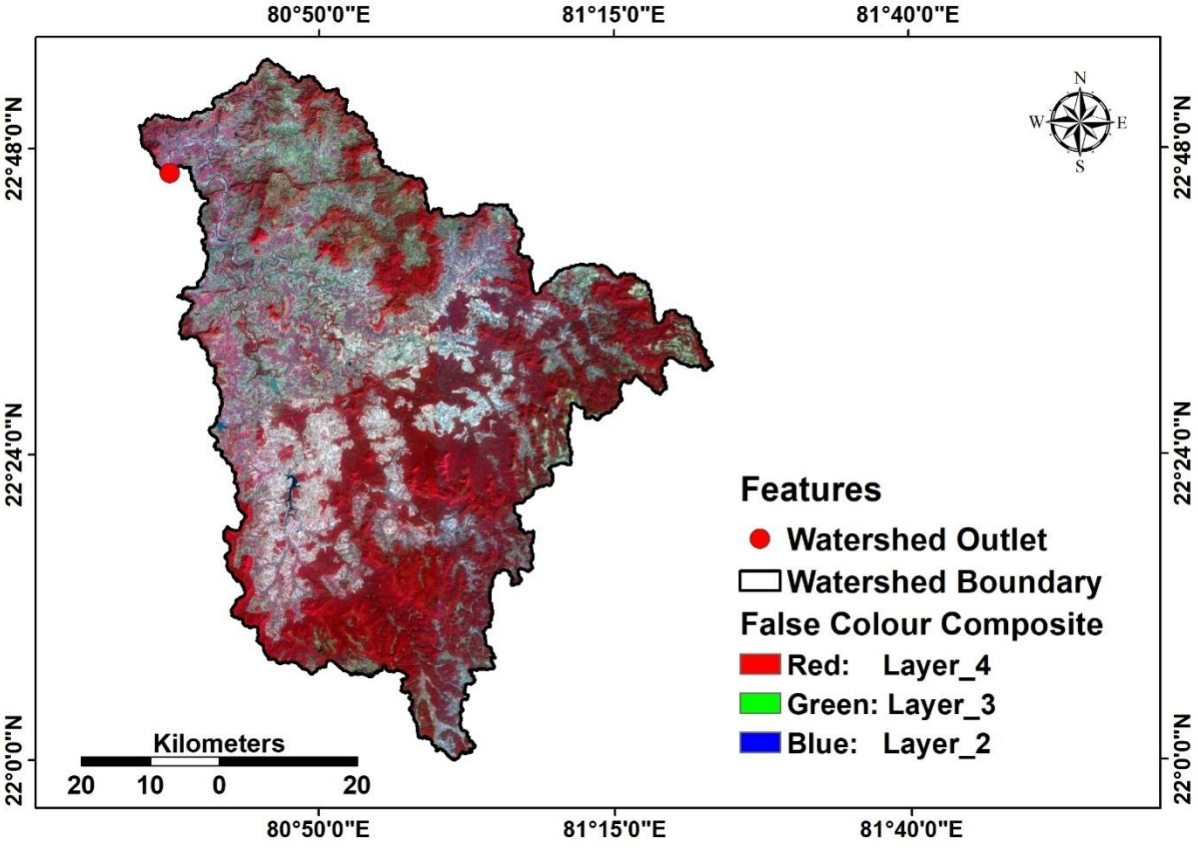

Fig. 2 False Colour Composite (FCC) image of the study area

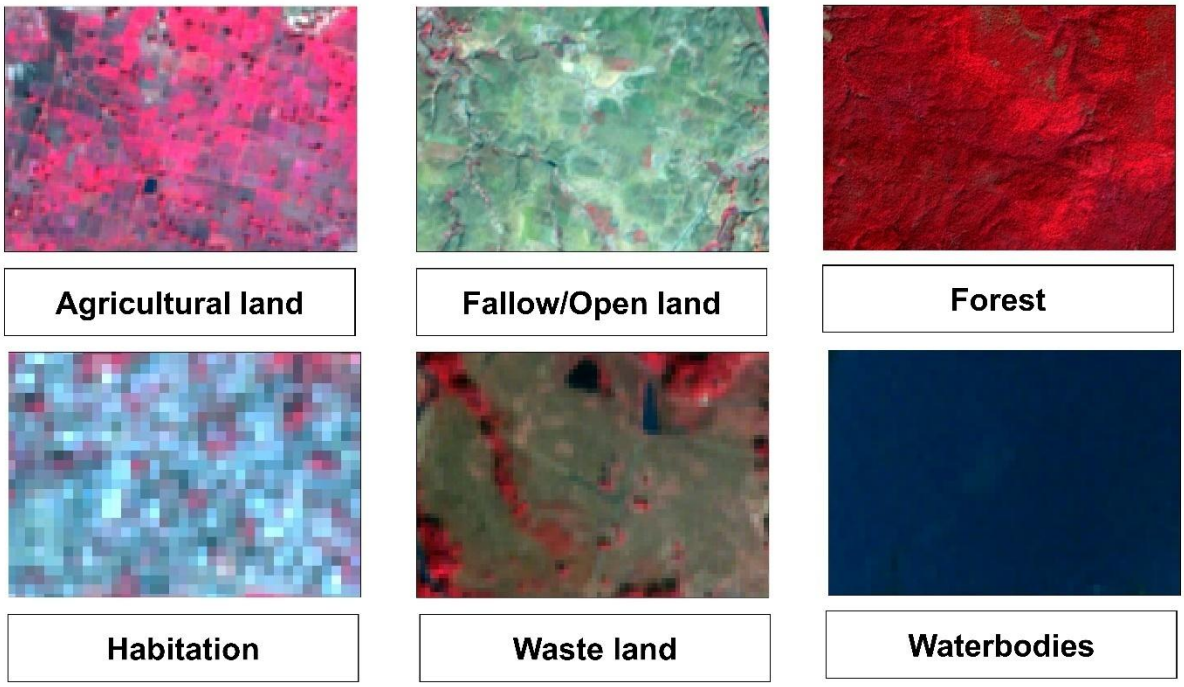

Fig. 3 Details of on-screen visual interpretation principles adopted for different LULC classes

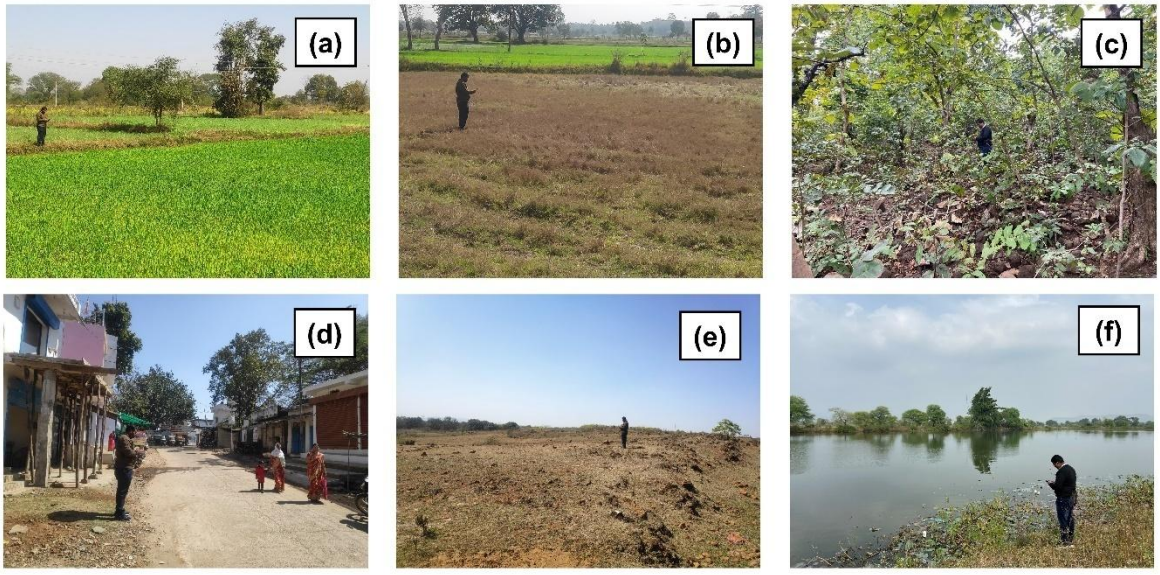

Fig. 4 Collection of reference (ground truth) data for different Land Use Land Cover (LULC) classes covered in Burhner River Watershed: (a) agricultural land, (b) fallow/open land, (c) forest, (d) habitation, (e) wasteland, (f) waterbodies

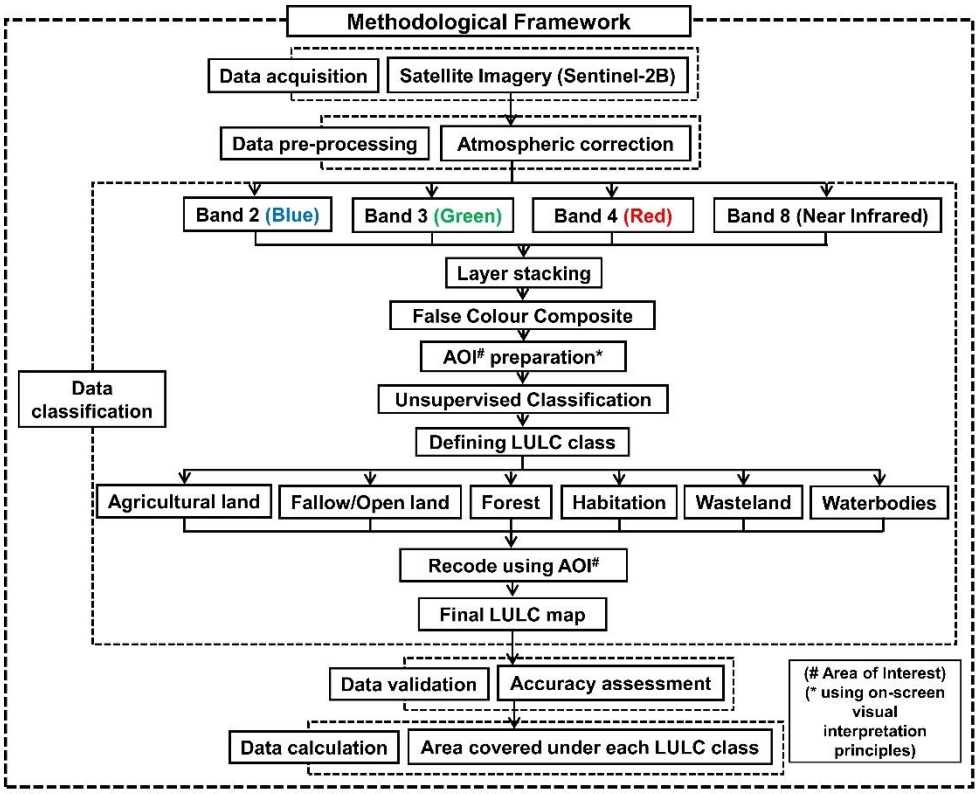

Fig. 5 Methodological framework used in LULC classification approach

2.4 Accuracy Assessment:

Accuracy assessment or validation is a significant step in the processing of remote sensing data [32]. The most common way to express the accuracy of classified image is by a percentage of the map area that has been correctly classified when compared with reference data or "ground truth" [33]. This statement can be justified by comparing the correctness of the classification generated by sampling the classified data expressed in the form of an error matrix (sometimes also referred as a confusion matrix or contingency table). An error matrix is a square array of numbers set out in rows and columns, which express the number of sample units assigned to a particular class in one classification relative to the number of sample units assigned to a particular class in another classification [34]. The row total in error matrix represents classified data whereas the column total represents reference or ground truth data.

An error matrix is a very effective way to represent the accuracy of produced thematic map, because it provides a clear way of deriving the individual accuracies of each class along with both the errors of inclusion (commission errors) and errors of exclusion (omission errors) present in the classification [35]. Commission error is simply defined as including an area into a class when it doesn't belong to that class whereas omission error occurs when an area is excluded from the class in which it truly does belong [34].

Apart from error of commission and error of omission, the error matrix is also used to compute other measures of accuracies such as overall accuracy, producer's accuracy and user's accuracy [33]. The overall accuracy for the image classification can be obtained by dividing the sum of the entries in the "from-to" agreement of the error matrix with the total number of the examined pixels (or sample units) in the classification [36]. Producer's and user's accuracies can be computed to determine the individual class accuracies in addition to computing the overall classification accuracy for the entire matrix. As the name suggests, the producer's accuracy signifies the interest of producer of classification that how well a certain area can be classified [37]. The user's accuracy is indicative of

the probability that a pixel classified on the map/image actually represents that category on the ground [33]. The error matrix also aides in generating kappa coefficient values which can be used as another measure of agreement or accuracy [38]. The generation of kappa coefficient ($\hat{k}$) has become a standard component of almost every accuracy assessment [37, 39, 40] and is a prime tool of most image analysis software packages that include accuracy assessment procedures [34].

For assessing the accuracy of classified map, a total number of 538 randomly distributed points were generated over the entire classified map in ArcGIS® 9.3 environment. The classified data was further compared for agreement with ground truth or reference data obtained from Google Earth Pro satellite data and field visit data (Fig. 4).

3. RESULTS AND DISCUSSION:

3.1 LULC Classification:

The land use land cover classification at large watershed scales is a heavy computational task yet is critical to landowners, researchers, decision makers and watershed planners enabling them to make informal decisions for varying objectives [15]. A total of six major LULC classes such as agricultural land (*i.e.*, crop land, agricultural plantation), fallow/open land, forest (*i.e.,* dense/closed and open category of evergreen forest), habitation (*i.e.,* built-up, rural), wasteland (*i.e.,* barren rocky, scrub land) and waterbodies (*i.e.,* streams, ponds, and reservoirs) were identified in Burhner river watershed.

Fig. 6 shows the classified LULC map of the study area. The LULC statistic of Burhner river watershed is shown in Table 2. It indicates that major portion of watershed area is covered by forest (*i.e.,* 53.01%) followed by fallow/open land (*i.e.,* 24%) and agricultural land (*i.e.,* 19.44 %) whereas very small area is covered by waste land (*i.e.,* 1.98%) and waterbodies (*i.e.,* 1.38%) and least area is covered by habitation (*i.e.,* 0.19%).

The percent area covered by different Land Use Land Cover (LULC) classes is represented by a bar chart in Fig. 7. The chart clearly indicates that a large percent of watershed area (*i.e.,* 24% or 950.256 km^2) falls under fallow/open land category showing underutilized potential of watershed land resources. Such available land resources can be further utilized for crop production, agricultural plantation, horticultural plantation and forest plantation purposes by watershed managers and local habitats of watershed. However utilization of such land resources is subjected to a number of constraining factors such as soil depth, topography, accessibility to the area and availability of water and human resources. But by using a proper planned scientific approach use of such land resources can play a key role in uplifting the socio economic conditions of local landowners, small and marginal farmers and local habitats of the study area.

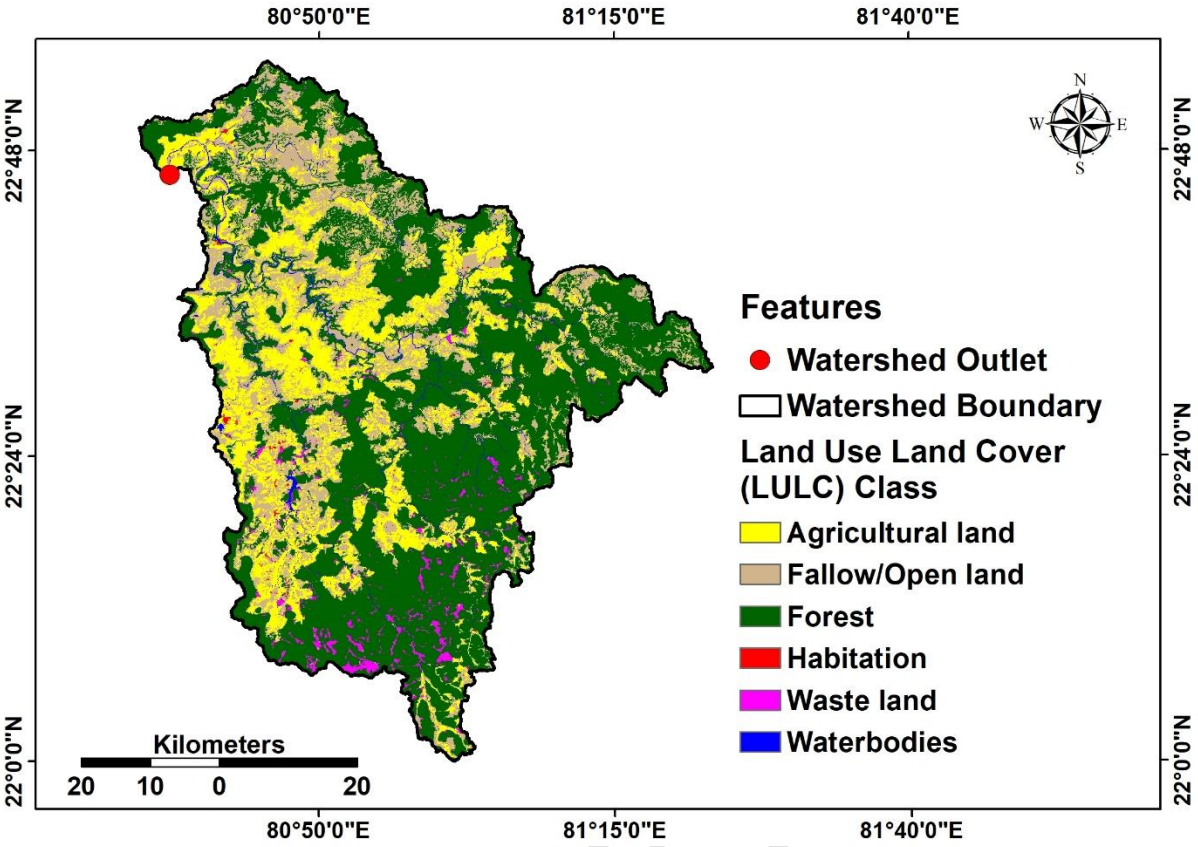

Fig. 6 LULC map of the study area

Table 2. Land Use Land Cover (LULC) statistic of Burhner river watershed

S.No.	Land Use Land Cover (LULC) Class	Area	Percent of total watershed area
		(km^2)	(%)
1	Agricultural land	769.787	19.44
2	Fallow/Open land	950.256	24.00
3	Forest	2099.118	53.01
4	Habitation	7.720	0.19

5	Waste land	78.219	1.98
6	Water bodies	54.713	1.38

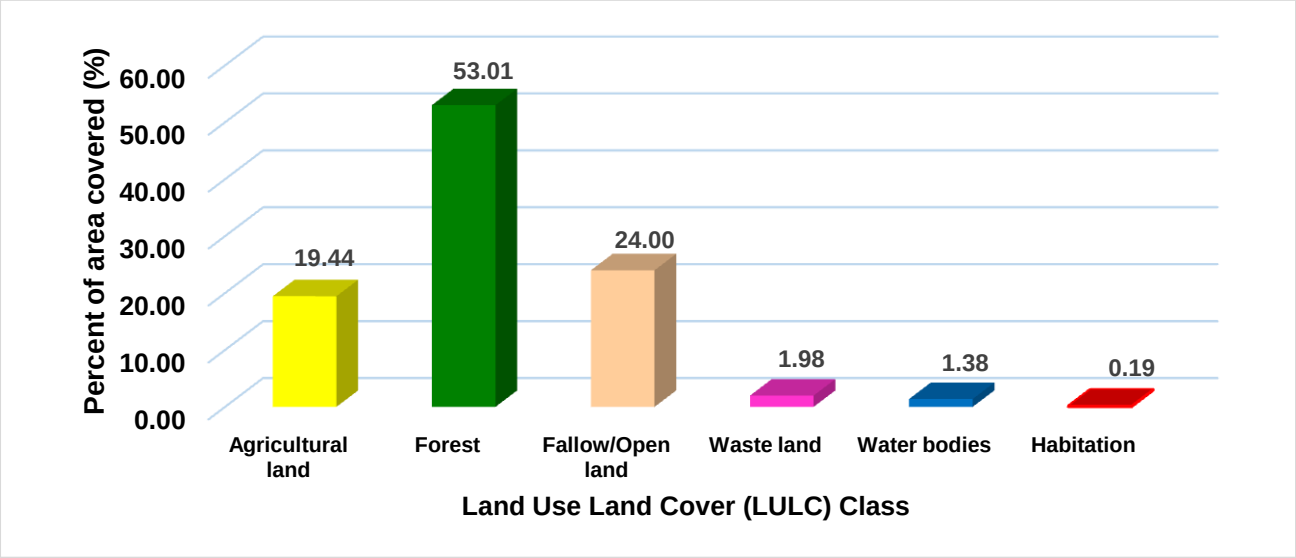

Fig. 7 Percent area covered by different Land Use Land Cover (LULC) classes

3.2 Accuracy Assessment:

To obtain the reliability of classified image, error matrix was generated (Table 3). The error matrix aided in assessing the overall accuracy, producer's accuracy, user's accuracy and kappa coefficient of the classified map using reference or ground truth data. The overall accuracy of the classified image was found as 95.72%. The producer's accuracy was calculated by dividing the principal diagonal (the agreement) by total number of sample points in that map class as specified by sum of the reference (ground truth) data (or column total) for that class. Table 3 clearly illustrates the process adopted for calculation of producer's accuracy of each class. The computation of producer's accuracy for different classes of classified image showed that agricultural land producer's accuracy was highest among all the classified classes (*i.e.,* 98.18%). It was further followed by forest (97.82%), habitation (96.42%), waterbodies (95.45%) and wasteland (94.11%). The least value of producer's accuracy was obtained for fallow land (90.07%) indicating a shift in large number of reference data sample points into other classified classes (disagreement) leading to high error of omission. By observing the error of omission (EO) for all the classes, it was evident that EO was highest for fallow/open land (9.93%), followed by wasteland (5.89%), waterbodies (4.55%), habitation (3.58%), forest (2.18%) and agricultural land (1.82%).

Apart from producer's accuracy, user's accuracy was also calculated for all the produced classes of the classified image (Table 3). The user's accuracy was highest for forest (98.25%), followed by fallow/open land (95.93%), agricultural land (94.73%), habitation (93.10%), waterbodies (87.5%) and wasteland (84.21%). The lower values of user's accuracy in case of waste land and waterbodies was due to the shift of sample points of classified data into other classes (disagreement) leading to high error of commission. A close observance of error of commission (EC) showed highest EC for waste land (15.79%), followed by water bodies (12.5%), habitation (6.90%), agricultural land (5.27%), fallow/open land (4.07%) and forest (1.75%).

The kappa coefficient ($\hat{k}$) of classified image was found as 0.94. A kappa coefficient value of $\hat{k}$ = 1 indicates a perfect agreement between the categories while a value of $\hat{k}$ = 0 indicates that the observed agreement equals the chance agreement [38]. A value greater than 0.75 indicates a very good to excellent agreement, while a value between 0.40 to 0.75 indicates a fair to good agreement [41]. A value of less than or equal to 0.4 indicates a poor agreement between the classification categories [42]. On the basis of such criteria, the value of $\hat{k}$= 0.94 in this case indicates good to excellent agreement.

Table 3: Error (Confusion) matrix

Confusion (Error) Matrix

Reference (Ground Truth) Data

Classified Data: LULC Class	AL	FO	FT	HT	WL	WB	Row Total
AL	108	5	0	0	0	1	114
FO	1	118	4	0	0	0	123
FT	0	3	225	0	1	0	229
HT	0	2	0	27	0	0	29
WL	0	1	1	1	16	0	19
WB	1	2	0	0	0	21	24
Column Total	110	131	230	28	17	22	538

Land Use Land Cover (LULC) Class		
Agricultural land	=	AL
Fallow/Open land	=	FO
Forest	=	FT
Habitation	=	HT
Waste land	=	WL
Water bodies	=	WB

Producer's Accuracy	User's Accuracy
AL = (108/110) × 100 = 98.18%	AL = (108/114) × 100 = 94.73%
FO = (118/131) × 100 = 90.07%	FO = (118/123) × 100 = 95.93%
FT = (225/230) × 100 = 97.82%	FT = (225/229) × 100 = 98.25%
HT = (27/28) × 100 = 96.42%	HT = (27/29) × 100 = 93.10
WL = (16/17) × 100 = 94.11%	WL = (16/19) × 100 = 84.21%
WB = (21/22) × 100 = 95.45%	WB = (21/24) × 100 = 87.5%

Overall Accuracy

$$= \{(108 + 118 + 225 + 27 + 16 + 21)/538\} \times 100$$

$$= (515/538) \times 100$$

$$= \mathbf{95.72\%}$$

Kappa coefficient

$$= \frac{(538 \times 515) - \{(110 \times 114) + \ldots.. + (22 \times 24)\}}{(538)^2 - \{(110 \times 114) + \ldots.. + (22 \times 24)\}}$$

$$= \mathbf{0.94}$$

4. CONCLUSION:

LULC information is increasingly in demand due to its ability to provide spatial distribution information at higher resolutions, which cannot be achieved by intensive ground surveys especially in regions where harsh topographic conditions pertain. The techniques of remote sensing and GIS thus find its applicability in continuous and precise monitoring of LULC patterns for different sorts of terrain units. The present study carried out in Burhner river watershed aims at performing the Land Use Land Cover (LULC) classification using high spatial resolution satellite imagery and its accuracy assessment. Accuracy assessment was executed by generating error matrix using random sample points created for classified image and reference (ground truth) data. A total number of six LULC classes were prepared during the classification process such as agricultural land, fallow/open land, forest, habitation, wasteland and water bodies. The highest percent of watershed area was covered by forest (*i.e.,* 53.01%) and least area was covered by habitation (*i.e.,* 0.19%). The classified map yielded an overall accuracy of 95.72%, with kappa coefficient $\hat{k}$ = 0.94 denoting good to excellent agreement. The producer's accuracy and user's accuracy also gave acceptable results. The LULC statistic revealed that a considerable portion of study watershed is covered under fallow/open land category indicating underutilized land resource potential of the watershed. Such land can be used for crop production and plantation purposes which can aid in uplifting the socioeconomic conditions of local habitats.

REFERENCES:

1. Sharma SK, Tignath S and Mishra SK. Morphometric analysis of drainage basin using GIS approach. JNKVV Res. J. 2008; 42(1):91-95.

2. Bagwan WA and Gavali RSS. Dam-triggered land use land cover change detection and comparison (transition matrix method) of Urmodi river watershed of Maharashtra, India: A Remote Sensing and GIS approach. Geol. Ecol. Landscapes. 2021; 1-9. https://doi.org/10.1080/24749508.2021.1952762.

3. Gajbhiye S, Sharma SK, Tignath S and Mishra SK. Development of geomorphological erosion index for Shakker watershed. J. Geol. Soc. India. 2015a; 86(3). https://doi.org./ http://dx.doi.org/10.1007/s12594-015-0323-3

4. Meshram SG and Sharma SK. 2018. Application of principal component analysis for grouping of morphometric parameters and prioritization of watershed. Hydrological Modeling, Select proceedings ICWEES-2016 (Springer). Editors: Singh V P, Yadav Shalini and Yadav Ramnarayan. 2018; 447-458.

5. Gajbhiye S, Singh SK, Sharma SK, Siddiqui AR and Singh PK. Assessing the effects of different land use on water quality using multi temporal Landsat data. Resource management, Development Strategies : A Geographical Perspective. 2015b; 337-348.

6. Patil RJ, Sharma SK, Tignath S and Sharma APM. Use of remote sensing, GIS and C^{++} for soil erosion assessment in Shakker river basin, India. Hydrol. Sci. J. 2017; 62(2): 217-231. https://doi.org/10.1080/02626667.2016.1217413

7. Suleiman MS, Wasonga OV, Mbau JS and Elhadi YA. Spatial and temporal analysis of forest cover change in Falgore Game Reserve in Kano, Nigeria. Ecol. Processes. 2017; 6(1): 1-13. https://doi.org/10.1186/s13717-017-0078-4

8. Palaniyandi M and Nagarathinam V. Land use/land cover mapping and change detection using space borne data. J. Indian Soc. Remote Sens. 1997; 25(1): 27-33. https://doi.org/10.1007/BF02995415

9. Sharma SK, Pathak R and Suraiya S. Prioritization of sub-watersheds based on morphometric analysis using remote sensing and GIS technique. JNKVV Res. J. 2012; 46(3):407-413.

10. Meshram SG, Singh VP, Kahya E, Alvandi E, Meshram C and Sharma SK. The feasibility of multi-criteria decision making approach for prioritization of sensitive area at risk of water erosion. Water Resour. Manage. 2020; 34(15): 4665-4685. https://doi.org/10.1007/s11269-020-02681-7

11. Saah D, Tenneson K, Matin M, Uddin K, Cutter P, Poortinga A et al. Land cover mapping in data scarce environments: challenges and opportunities. Front. Environ. Sci. 2019; 7:150. https://doi.org/10.3389/fenvs.2019.00150

12. Sharma SK, Yadav A and Gajbhiye S. Remote sensing and GIS approach for prioritization of watershed. LAMBERT Academic Publishing. 2014.

13. Rao JH, Patle D and Sharma SK. 2020b. Remote sensing and GIS technique for mapping land use/land cover of Kiknari watershed. Indian J. Pure Appl. Biosci. 2020b; 8(6): 455-463. https://doi.org/10.18782/2582-2845.8458

14. Ponnana RK, Sankar GJ, Elakurthi S, Bendalam S. A Geo-Spatial approach to the land use / land cover mapping of the Kandivalasa river basin Vizianagaram district Andhra Pradesh, India. Int. J. Adv. Res. Eng. Technol. 2021; 12(3): 280–290. https://doi.org/10.34218/IJARET.12.3.2021.028

15. Yang D, Fu CS, Smith AC and Yu Q. Open land-use map: a regional land-use mapping strategy for incorporating OpenStreetMap with earth observations. Geo-spatial Inf. Sci. 2017; 20(3): 269–281. https://doi.org/10.1080/10095020.2017.1371385

16. Rujoiu-Mare MR and Mihai BA. Mapping land cover using remote sensing data and GIS techniques: A case study of Prahova Subcarpathians. Procedia Environ. Sci. 2016; 32: 244–255. https://doi.org/10.1016/j.proenv.2016.03.029

17. Rao JH, Patle D and Dubey S. Implementation of morphometric analysis in prioritizing sub-watersheds: a remote sensing and GIS aspect. Indian J. Pure Appl. Biosci. 2020a; 8(4): 318-329.

18. Biswas S, Sudhakar S and Desai VR. Prioritisation of subwatersheds based on morphometric analysis of drainage basin: a remote sensing and GIS approach. J. Indian Soc. Remote Sens. 1999; 27(3): 155-166.

19. Dubey S, Rao JH and Patle D. Morphometric analysis and prioritization of sub watersheds of Umar nala watershed, Madhya Pradesh using geospatial technique. Int. J. Agric. Environ. Biotechnol. 2020; 13(3): 269-274.

20. Patle D, Rao JH and Dubey S. Morphometric analysis and prioritization of sub-watersheds in Nahra watershed of Balaghat district, Madhya Pradesh: a remote sensing and GIS perspective. J. Exp. Biol. Agric. Sci. 2020a; 8(4): 447-455.

21. Manandhar R, Odehi IOA and Ancevt T. Improving the accuracy of land use and land cover classification of landsat data using post-classification enhancement. Remote Sens. 2009; 1(3): 330–344. https://doi.org/10.3390/rs1030330

22. Basukala AK, Oldenburg C, Schellberg J, Sultanov M and Dubovyk O. Towards improved land use mapping of irrigated croplands: performance assessment of different image classification algorithms and approaches. Eur. J. Remote Sens. 2017; 50(1): 187–201. https://doi.org/10.1080/22797254.2017.1308235

23. Lo CP and Choi J. A hybrid approach to urban land use/cover mapping using Landsat 7 Enhanced Thematic Mapper Plus (ETM+) images. Int. J. Remote Sens. 2004; 25(14): 2687-2700.

24. Sharma SK, Seth NK, Tignath S and Pandey RP. Use of Geographical Information System in hypsometric analysis of watershed. J. Indian Water Resour. Soc. 2011a; 31(3-4): 28-32.

25. Sharma SK, Gajbhiye S, Nema RK and Tignath S. Assessing vulnerability to soil erosion of a watershed of Narmada basin using remote sensing and GIS. Int. J. Sci. Innovative Eng. Technol. 2015; 1

26. Palanichamy A. Land use / land cover mapping in analysis of Tiruchirappali district Tamilnadu using geoinformatics. Int. J. Latest Trends Eng. Technol. 2018; 9(4): 161-165.

27. Sharma SK, Seth NK, Tignath S and Shukla JP. Land use/land cover mapping of Gusuru river using remote sensing and GIS technique. JNKVV Res. J. 2011b; 45(1): 125-128.

28. Patle D, Rao JH, and Sharma SK. Land use/land cover mapping of Nahra nala watershed using SENTINEL-2B imagery. Int. J. Agric. Environ. Biotechnol. 2020b; 13(4): 439-446.

29. Rao JH, Hardaha MK and Vora HM. The water footprint assessment of agriculture in Banjar river watershed. Curr. World Environ. 2019; 14(3): 476 - 488.

30. Pai DS, Rajeevan M, Sreejith OP, Mukhopadhyay B and Satbha NS. Development of a new high spatial resolution (0.25× 0.25) long period (1901-2010) daily gridded rainfall data set over India and its comparison with existing data sets over the region. Mausam. 2014; 65(1): 1-18.

31. Rao JH, Sharma SK, Awasthi MK, Pyasi SK and Pandey SK. Morphometric analysis of Burhner river watershed using remote sensing and GIS technique. Int. J. Agric. Environ. Biotechnol. 2021; 14(04): 585-599.

32. Rwanga SS and Ndambuki JM. Accuracy assessment of land use/land cover classification using remote sensing and GIS. Int. J. of Geosci. 2017; 8(04): 611–622. https://doi.org/10.4236/ijg.2017.84033

33. Story M and Congalton RG. Accuracy assessment: a user's perspective. Photogramm. Eng. Remote Sens.1986; 52(3): 397-399.

34. Congalton RG and Green K. Assessing the accuracy of remotely sensed data principles and practices, Third Edition. In CRC Press. 2019.

35. Congalton RG and Green K. Practical look at the sources of confusion in error matrix generation. Photogramm. Eng. Remote Sens. 1993; 59(5): 641–644.

36. Islam K, Jashimuddin M, Nath B and Nath TK. Land use classification and change detection by using multi-temporal remotely sensed imagery: The case of Chunati wildlife sanctuary, Bangladesh. Egypt. J. Remote Sens. Space Sci. 2018; 21(1): 37-47.

37. Congalton RG. A review of assessing the accuracy of classifications of remotely sensed data. Remote Sens. Environ. 1991; 37(1): 35-46.

38. Cohen J. A coefficient of agreement for nominal scales. Educ. and Psychol. Meas. 1960; 20(1): 37-46.

39. Rosenfield GH, Fitzpatrick-Lins K and Ling HS. Sampling for thematic map accuracy testing. Photogramm. Eng. Remote Sens.1982; 48(1): 131-137.

40. Hudson W and Ramm C. Correct formulation of the kappa coefficient of agreement. Photogramm. Eng. Remote Sens. 1987; 53(4): 421-422.

41. Pandey A, Chowdary VM and Mal BC. Identification of critical erosion prone areas in the small agricultural watershed using USLE, GIS and remote sensing. Water Resour. Manage. 2007; 21(4): 729-746.

42. Manserud RA and Leemans R. Comparing global vegetation maps with the Kappa statistic. Ecol. Modell.1982; 62(4): 275-293.